Journal of Applied Polymer Science

Synthesis and thermal, optical and morphological characterization of oligomeric polyamides based on thiophene and alkyl/phenyl-silane moieties. Study of the electrospun deposition process

Ignacio A. Jessop,[1] Alain Tundidor-Camba,[2] Claudio A. Terraza,[2] Carmen M. González-Henríquez,[3,4] Luis H. Tagle[2]

[1]Facultad de Ciencias, Universidad de Tarapacá, Av. General Velásquez 1775, Arica, Chile
[2]Facultad de Química, Pontificia Universidad Católica de Chile, Santiago, P.O. Box 306, Chile
[3]Facultad de Ciencias Naturales, Matemáticas y del Medio Ambiente, Universidad Tecnológica Metropolitana, P.O. Box 9845, Correo 21, Santiago, Chile
[4]Programa Institucional de Fomento a la Investigación, Desarrollo e Innovación, Universidad Tecnológica Metropolitana, P.O. Box 9845, Correo 21, Santiago, Chile
Correspondence to: C. A. Terraza (E-mail: cterraza@uc.cl)

ABSTRACT: Polyamides were synthesized from a thiophene-containing diamine by direct polycondensation with organosilane acyl dichlorides. The obtained polymers had good solubility in common organic solvents and THF, with $TDT_{10\%}$ values upper than 400 °C and T_g between 150 and 180 °C. Combination of these properties reveals that the processability of the polymers was increased with respect to traditional aromatic polyamides. Inherent viscosity values and SEC analysis indicated low molecular weight species. Samples showed high visible transparency and bandgap values associated to insulating materials. Polymer solutions were deposited using electrospun technique and their surface properties were studied by SEM. Spheres were created according to electric field applied during deposition process. Low molecular weight and conductivity prevent charge accumulation in the surface hindering fibers generation. © 2016 Wiley Periodicals, Inc. J. Appl. Polym. Sci. **2016**, *133*, 43702.

KEYWORDS: morphology; polyamides; properties and characterization; thermal properties

Received 3 December 2015; accepted 22 March 2016
DOI: 10.1002/app.43702

INTRODUCTION

Aromatic polyamides (PAs) are a class of high-performance polymers that have been widely used in technological applications, in some cases being substituted for ceramics and metals. Some applications are found in the field of the automotive/aerospace components, military devices, microelectronic industry development, and membrane materials, due to their outstanding mechanical, thermal stability, chemical resistance, low flammability, and hydrolytic stability features as well as their permselective properties, particularly in reverse osmosis.[1–6] However, chain stiffness and intermolecular hydrogen bonding between amide groups, limit their solubility in common organic solvents together with high transition temperature, making their processability difficult.[7]

Some strategies to improve processing properties of aromatic PAs includes the introduction of specific substituents on the aromatic rings, e.g., bulky substructures or side groups, which favors the separation of the polymer chains and hinder molecular packing or crystallization.[6–8] In further details, the incorporation of fluorine as trifluoromethyl groups reduces interchain interaction and increases the material optical clarity[9,10]; linear aliphatic and nonlinear rigid alicyclic/aromatic structures or asymmetric monomer could affect the molecular ordering in the system.[7,11] The introduction of flexible moieties, such as diamines, diacids and silane groups, into the polymer backbone should reduce the chain stiffness, increasing the solubility and decreasing the glass transition temperature without sacrificing the final thermal stability of the material.[12,13]

As previously mentioned, aromatic PAs have been widely used as engineering materials.[7] The internal structure-conformation and crystallinity are determined mainly by hydrogen bonding (amide groups-polar) and Vander Waals forces (methylene chains-apolar), interactions that affect their polymer length and, also, their dielectric properties. This type of material is widely applied, like other polymers such as polystyrene, polyacrylonitrile, and several polycarbonates, in electrospinning.[14–20] Thus,

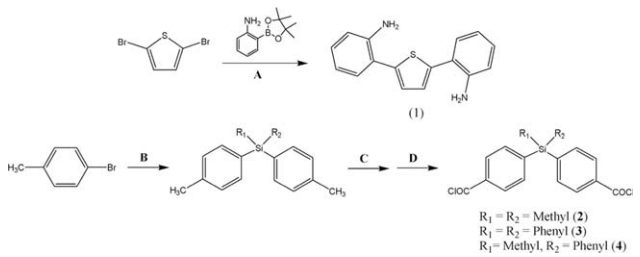

Scheme 1. Synthetic route for the synthesis of the thiophene-containing diamine and the organosilane monomers. (A) $Pd(PPh_3)_2Cl_2$, 1 M K_2CO_3, 1,4-dioxane, inert atmosphere, reflux, 48 h. (B) 1) Li-Et_2O, r.t., 2) R_1,R_2SiCl_2-Et_2O. (C) 1) $KMnO_4$, pyridine-H_2O, 90 °C, 2) HCl. (D) $SOCl_2$, pyridine, r.t.

electrospun is a technique employed for the formation and deposition of ordered nano- and micro-structures, being able to control their diameter, spatial distribution, porosity, and orientation. The conformation of these types of micro-/nano-structures as layers produces in some cases materials with porous surface. Basically, this technique consists in the application of a powerful electric field to a metal capillary that ejects the polymer solution at a controlled flow. Dissolved polymer surface charges produce collapsed polymer structures that, according to potential difference, are collected by a ground connected plate. Also, due to the high velocity and temperature acquired during deposition, the solvent is evaporated producing a solid polymeric deposition.[21–23]

Previously, our research group has described the synthesis and characterization of several PAs using the Yamazaki-Higashi polycondensation technique. These polymers contain silicon and/or germanium and several organic substituents into their main chain favoring the flexibility of the system, allowing chain folding. These characteristics make these polymers suitable for manipulation generating possible technological implementation.[24–30]

In this study, the synthesis of a new series of polyamides based on thiophene-dianiline unit and alkyl/phenyl-silane monomers is reported. The product was characterized by spectroscopic, thermal and optical methods. These polymers were dissolved and then deposited over solid substrates using electrospun technique. This procedure was performed focused specially in the symmetry/asymmetric effect of the substitutions on the silicon atom. In order to visualize these structures, SEM studies were accomplished. The obtained results showed that the high voltage applied during the deposition process, their polymeric structure, concentration and the solvent nature used affect the surface morphology of the samples. Thus, spheres with a certain concavity were obtained in most of the compounds with diameters around 0.8–4.5 μm.

EXPERIMENTAL

Materials

Anhydrous *N,N′*-dimethylacetamide (DMAc), was purchased from Aldrich Chemical (Milwaukee, WI). 4,4′-(Dimethylsilanediyl)dibenzoyl chloride (**2**), 4,4′-(diphenylsilanediyl)dibenzoyl chloride (**3**), and 4,4′-[methyl(phenyl)silanediyl]dibenzoyl chloride (**4**) were synthesized following a procedure already reported elsewhere by our research group.[25] 2,2′-(Thiophene-2,5-diyl)dianiline (**1**) was previously prepared.[31] All other reagents and solvents were analytical grade commercially available and used as received.

Instrumentation

FT-IR spectra of the polymers dispersed in KBr pellets were recorded on a Bruker Vector 22 spectrometer. ^{1}H, ^{13}C and ^{29}Si NMR spectra were recorded on a 400 MHz Bruker spectrometer. Elemental analyses were carried out on a Fisons EA 1108-CHNS-O equipment. Viscosimetric measurements were carried out in a Desreux-Bischof type dilution viscosimeter at 25 °C using *N*-methyl-2-pyrrolidone (NMP) as solvent ($c = 0.5$ g dL^{-1}). SEC analyses were carried out at 25 °C using a system composed of three PLgel 5μ Mixed-C columns placed in series, refractive index (Optilab DSP) and light-scattering (EA-02 Dawn Eos Enhanced Optical System) detectors and Knauer pump model 14163. THF was used as eluent (8 mg mL^{-1}). Thermogravimetric analysis (TGA) was performed in a TGA/DSC 1 Star e System Mettler Toledo thermobalance heating the samples from 20 °C to 900 °C at a rate 10 °C min^{-1} under nitrogen flow. Glass transition temperature (T_g) was measured by differential scanning calorimetry (DSC) technique on a Mettler Toledo, DSC 822e Differential Scanning Calorimetric from the second heating run. UV-Vis optical transmission spectra were obtained on a UV-3101PC UV-vis-NIR scanning spectrophotometer using 1 cm optical path quartz cells. Absorption spectra were recorded at 25 °C between 200–800 nm on a Perkin Elmer Lambda 35 spectrophotometer with 1.0 slit, 480 nm min^{-1} scan rate and using ~ 1 mg PA mL^{-1} THF solution in 0.7 mL optic cells. Photoluminescence spectra were recorded at room temperature on a Perkin Elmer L55 spectrofluorimeter, using an excitation wavelength of 360 nm and 10 ex slit and 300 nm min^{-1} scan rate. To this purpose, ~ 0.15 mg mL^{-1} PAs solutions were prepared in THF. Electrospun system was a home-made equipment that uses a high voltage power supply model AU-50R 0.6, 30 W, 50 kV maximum output voltage, 0.6 mA maximum output current (Matsusada Precision Inc.). A Syringe pump, model TJ-1A/L0107-1A (controller type/drive unit type) with only infusion working mode (Longer Syringe Pump) and a Hamilton Syringe of 250 μL (Model 725 N), nominal outer/inner diameter: 0.72 mm/0.15 mm, respectively. Polymers micrographs were

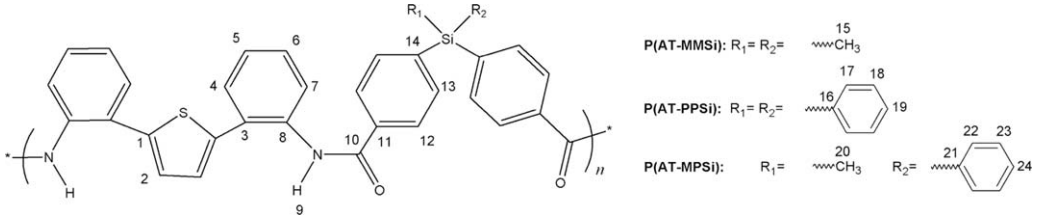

Scheme 2. General synthesis for the NMR signals assignation.

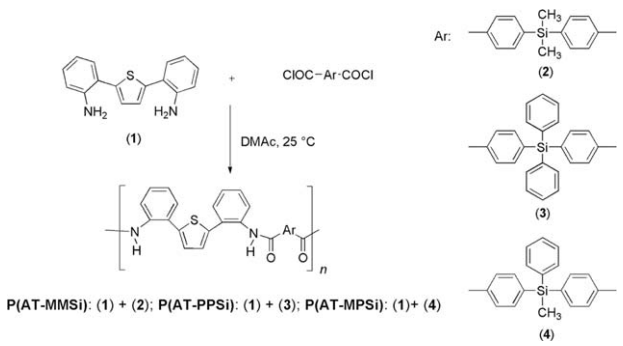

Scheme 3. General synthesis of polyamides from thiophene-containing diamine and silylated aromatic acid chlorides.

obtained on a Scanning Electron Microcopy (SEM), Carl Zeiss, model EVO–MA 10. Argon sputter coater (Cressington, 108 AUTO) coupled with a high-resolution film thickness monitor (Cressington, MTM-20) using a rotary tilting stage (with 90 rpm frequency) was utilized. A gold deposit of 3.6 ± 0.01 nm over the polymeric sample was applied using 20 mA, 0.08 mbar (argon pressure) and ~ 7 cm working distance. Gold target purity was 99.99% (Ø 0.57 mm × 0.2 mm), extra-pure argon (4N8) was also used. The deposited metal prevents charge effects during SEM measurements, a common problem in dielectric samples.

Monomers Synthesis

2,2′-(Thiophene-2,5-diyl)dianiline (**1**) monomer was synthesized by Jessop *et al.* via Suzuki-Miyaura cross-coupling reaction.[31,32] Briefly, 2,5-dibromothiophene was reacted with 2-(4,4,5,5-tetramethyl-1,3,2-dioxaborolan-2-yl)aniline in presence of $Pd[PPh_3]_2Cl_2$ as catalyst, K_2CO_3 as base and 1,4-dioxane as solvent under nitrogen atmosphere. The diamine was purified by column chromatography and then recrystallized from EtOH/H_2O to afford 75% yield.

Organosilane monomers, 4,4′-(dimethylsilanediyl)dibenzoyl chloride (**2**), 4,4′-(diphenyl silanediyl)dibenzoyl chloride (**3**), and 4,4′-(methyl(phenyl)silanediyl)dibenzoyl chloride (**4**), were prepared according to previously described procedures.[25,33] *p*-Bromotoluene reacts first with lithium and then with dichloro-R_1R_2-silane. Ditolyl derivatives were oxidized to the corresponding dicarboxylic acid using $KMnO_4$ in basic medium, followed by reaction with thionyl chloride (Scheme 1).

Polymers Synthesis

To a three-necked round-bottom flask equipped with a mechanical stirrer, 1.00 mmol of diamine **1**, 1.0 mL of dry DMAc and 0.2 mL of pyridine were added. After complete dissolution, it was cooled into an ice-water bath and then 1.00 mmol of silylated acid dichloride **2** and 1.0 mL of dry DMAc were added. The ice-water bath was removed when the acid dichloride was totally dissolved. The mixture was then stirred at room temperature for 6 h. The resulting mixture was poured into 300 mL of water with stirring. **P(AT-MMSi)** was obtained as a white solid that was filtered, thoroughly washed with water and dried at 100 °C for 12 h. **P(AT-PPSi)** and **P(AT-MPSi)** were obtained following the same procedure replacing the silylated acid dichloride **2** by **3** and **4**; respectively. The samples were structurally characterized by elemental analysis, FT-IR and NMR techniques. Scheme 2 shows the positions used in the NMR signals assignation.

P(AT-MMSi)

Yield: 99%. FT-IR (KBr): $\upsilon = 3407$ (N—H), 3065, 3018 (C—H arom. phenyl), 2953 (C—H aliph.), 1672 (C═O), 1581, 1517, 1493 (C═C arom.), 1438 (Si—C arom.), 1231 (Si—C aliph.), 754 cm^{-1} (C—H arom. thiophene). ^1H NMR (400 MHz, DMSO-d_6, δ): 10.07 (s, $2H^9$), 7.89 (d, $J = 7.4$ Hz, $4H^{13}$), 7.61 (d, $J = 7.4$ Hz, $4H^{12}$), 7.55 (d, $J = 6.8$ Hz, $2H^7$), 7.40 (d, $J = 7.7$ Hz, $2H^6$), 7.37 (s, $2H^2$), 7.32 (d, $J = 6.4$ Hz, $2H^4$), 7.25 (d, $J = 6.3$ Hz, $2H^5$), 0.58 ppm (s, $6H^{15}$). ^{13}C NMR (400 MHz, DMSO-d_6, δ): 165.91 (C_{10}), 141.69 (C_{11}), 140.20 (C_1), 134.98 (C_8), 134.26 (C_{14}), 133.94 (C_{12}), 130.76 (C_3), 129.24 (C_6), 128.80 (C_2), 128.44 (C_4), 127.99 (C_{13}), 126.90 (C_5), 126.37 (C_7), −2.94 ppm (C_{15}). ^{29}Si NMR (400 MHz, DMSO-d_6, δ): −7.57 ppm. Anal. calcd. for $C_{32}H_{26}N_2SO_2Si$; (530.72): C 72.42, H 4.94, N 5.28; found: C 72.99, H 4.56, N 5.12.

P(AT-PPSi)

Yield: 99%. FT-IR (KBr): $\upsilon = 3406$ (N—H), 3066, 3046, 3018 (C—H arom. phenyl), 1673 (C═O); 1579, 1515, 1491 (C═C arom.), 1429 (Si—C arom.), 755 cm^{-1} (C—H arom. thiophene). ^1H NMR (400 MHz, DMSO-d_6, δ): 10.16 (s, $2H^9$), 7.94 (d,

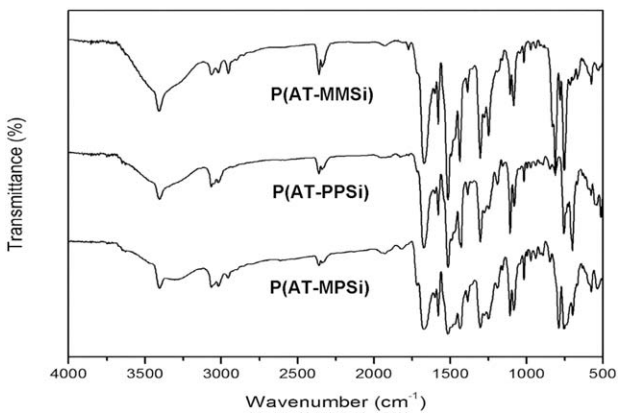

Figure 1. FT-IR spectra of silylated-polyamides.

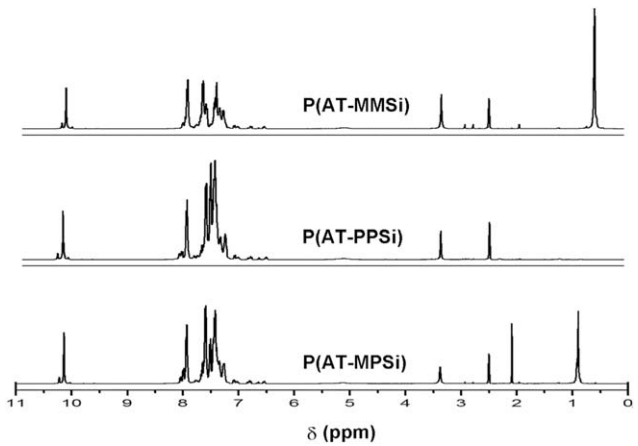

Figure 2. ^1H RMN spectra of **P(AT-MMSi)**, **P(AT-PPSi)**, and **P(AT-MPSi)**.

Table I. Inherent Viscosity and SEC Results for PAs

	η_{inh}[a] (dL/g)	M_n[b] (g/mol)	Repetitive units[c]	M_w (g/mol)	Repetitive units[c]	M_w/M_n[d]
P(AT-MMSi)	0.15	3065	6	5115	10	1.67
P(AT-PPSi)	0.16	4065	6	7025	11	1.73
P(AT-MPSi)	0.16	3340	6	5940	10	1.78

[a] Measured in NMP (0.5 g/dL at 25 °C).
[b] Analysis developed at 25 °C using THF as eluent (8 mg/mL).
[c] Repetitive units number calculated according with the molecular weight of them (Polymer Synthesis section).
[d] Polydispersity index.

$J = 7.9$ Hz, $4H^{13}$), 7.59 (d, $J = 7.3$ Hz, $4H^{12}$), 7.51 (m, $4H^{6,7}$), 7.48-7.37 (m, $12H^{2,17-19}$), 7.34 (d, $J = 5.9$ Hz, $2H^{4}$), 7.25 ppm (d, $J = 5.0$ Hz, $2H^{5}$). ^{13}C NMR (400 MHz, DMSO-d_6, δ): 165.85 (C_{10}), 140.19 (C_1), 137.25 (C_{11}), 135.85 (C_{12}), 135.63 (C_8), 134.17 (C_{14}), 132.58 (C_{16}), 130.76 (C_3), 130.14 (C_{17}), 129.23 (C_6), 128.73 (C_2), 128.33 (C_4), 128.29 (C_{18}), 127.97 (C_{13}), 127.16 (C_{19}), 126.94 (C_5), 126.40 ppm (C_7). ^{29}Si NMR (400 MHz, DMSO-d_6, δ): −15.06 ppm. Anal. calcd. for $C_{42}H_{30}N_2SO_2Si$; (654.86): C 77.03, H 4.62, N 4.28; found: C 76.88, H 4.49, N 4.40.

P(AT-MPSi)

Yield: 99%. FT-IR (KBr): $\upsilon = 3406$ (N—H), 3065, 3017 (C—H arom. phenyl), 2955 (C—H aliph.), 1673 (C═O), 1581, 1515, 1494 (C═C arom.), 1436 (Si—C arom.), 1222 (Si-C aliph.), 754 cm^{-1} (C—H arom. thiophene). ^1H NMR (400 MHz, DMSO-d_6, δ): 10.14 (s, $2H^{9}$), 7.94 (d, $J = 7.4$ Hz, $4H^{13}$), 7.59 (d, $J = 7.4$ Hz, $4H^{12}$), 7.51 (m, $4H^{6,7}$), 7.49–7.38 (m, $9H^{2,4,22-24}$), 7.27 (d, $J = 7.1$ Hz, $2H^{5}$), 0.89 ppm (s, $3H^{20}$). ^{13}C NMR (400 MHz, DMSO-d_6, δ): 165.89 (C_{10}), 140.28 (C_1), 139.45 (C_{11}), 135.32 (C_8), 134.88 (C_{12}), 134.69 (C_{14}), 134.23 (C_{21}), 130.77 (C_3), 129.82 (C_{22}), 129.24 (C_6), 128.77 (C_2), 128.57 (C_{24}), 128.18 (C_4), 128.14 (C_{23}), 127.99 (C_{13}), 127.03 (C_5), 126.40 (C_7), −4.04 ppm (C_{20}). ^{29}Si NMR (400 MHz, DMSO-d_6, δ): −11.20 ppm. Anal. calcd. for $C_{37}H_{28}N_2SO_2Si$; (592.79): C 74.97, H 4.76, N 4.74; found: C:74.01, H 4.57, N 4.82.

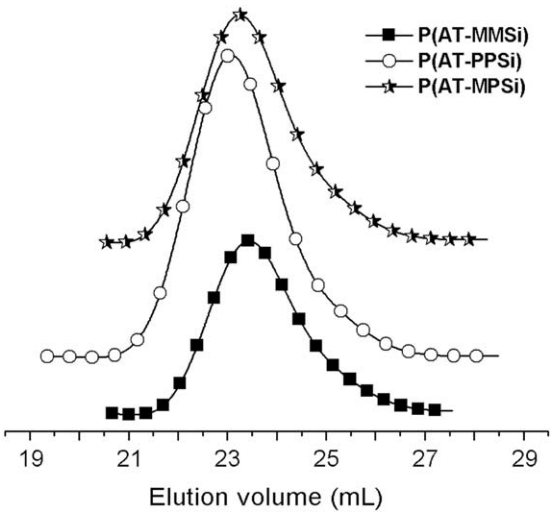

Figure 3. Size-exclusion chromatography (SEC) of PAs.

Polymer Deposition Using Electrospinning Technique. SEM Images

30 mg of each polymer was dissolved in 200 μL THF. This solution was placed into a Hamilton syringe (725N, volume 250 μL, needle size 22s ga (bevel tip), and needle long 51 mm). Syringe extrude flow rate (1.2 μL/min) was controlled using an appropriate pump; deposition time over copper sheets (1 cm^2) was 2 min for each sample. The applied voltage to deposit samples was ca. 20 kV (∼ 0.08 mA). The substrate was placed over a conductive copper plate, which is placed at 4 cm from syringe needle tip. For obtaining SEM images, it was necessary to recover the polymer film with gold in order to reduce sample charging, avoiding possible polymer melting due to temperature increase according to current application during SEM measurements.

RESULTS AND DISCUSSION

Polymer Synthesis

Synthesis of the monomers was conducted following established procedures and their purity was determined by spectroscopic analysis and melting point range. From these compounds, direct polymerization reaction was carried out using an equimolar mixture of the diamine and the respective silicon-containing dichloride derivative in dry DMAc solution at 25 °C, which allows obtaining the corresponding polyamide (Scheme 3). In all cases, the polymers were obtained as white solids in quantitative yield.

PAs Spectroscopic Characterization

Polymers structure was verified by elemental analysis and spectroscopic techniques (FT-IR and NMR). All infrared spectra (Figure 1) exhibited characteristic absorbance bands at about 3400 and 1670 cm^{-1} corresponding to the N—H and C═O stretching of the amide group, respectively. Also, C—H stretching vibrations of the different aromatic phenyl rings were observed between 3100 and 3000 cm^{-1}. **P(AT-MMSi)** and **P(AT-MPSi)** spectra showed a distinctive band at about 2950 cm^{-1} which is assigned to C—H stretching of methyl groups. Likewise, these polymers display the Si—C aliphatic bond vibration at 1230 cm^{-1}. On the other hand, a distinctive signal was observed between 1494 and 1438 cm^{-1} for all samples that reveals the Si—C aromatic stretching vibration. Finally, an intensive absorption band at 755 cm^{-1} was evidenced. This signal is generated by the C—H out of plane bending from the 2,5-disustituted thiophene moiety.[34]

^1H NMR spectra of PAs are seen in Figure 2. The peaks at about 10 ppm are due to the resonance of N—H amidic protons

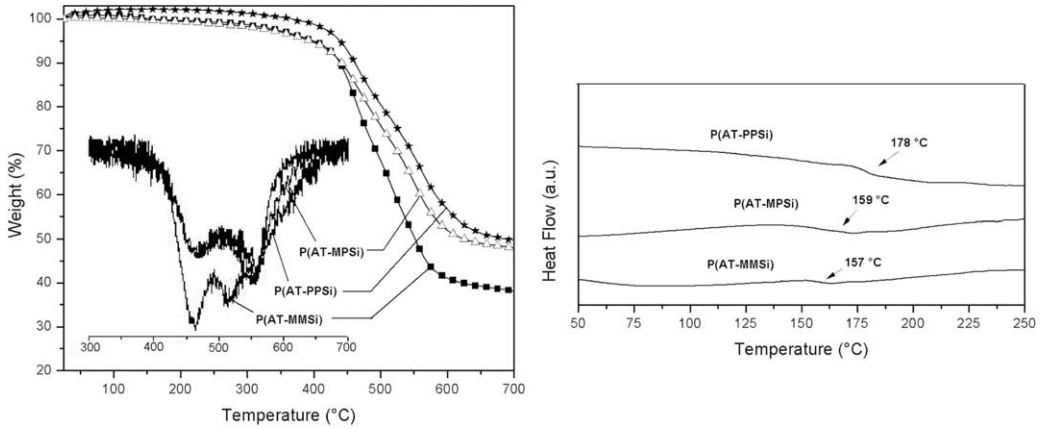

Figure 4. Thermograms (left) and DSC curves (right) of PAs.

that can be used to verify the condensation reaction. The signals between 8.00 and 7.15 ppm are assigned to protons from aromatic rings of the polymers backbone (phenyl and thiophene moieties). The singlet signals at 0.58 and 0.89 ppm are ascribed to protons of methyl groups in **P(AT-MMSi)** and **P(AT-MPSi)**, respectively. The shift at high magnetic field with respect to a normal aliphatic methyl group is due to the silicon atom effect. The electronegativity of the latter element is lower than the carbon atom and therefore its environment is enriched in electronic density. The same effect is also clearly observed for the methyl carbon in the ^{13}C NMR spectra. This last analysis revealed the presence of the carbonyl carbon of the amide groups at ca. 165 ppm. The shifts of the silicon nuclei (^{29}Si NMR analysis) agree with their electronic environment. Thus, when a methyl group is replaced for a phenyl moiety, the silicon resonance is shifted toward higher fields due the electronic behavior of the rings.[35]

PAs Inherent Viscosity, Molecular Weight, and Solubility

Table I summarizes the inherent viscosity of polyamides. This parameter was determined in NMP using a 0.5 g dL^{-1} solution at 25 °C. The range of values for the inherent viscosity (0.15–0.16 dL g^{-1}) and the wide compatibility with the tested common organic solvents shown by the polymers indicate a low molecular weight for the samples. These observations were corroborated by SEC analysis (Table I). The recovered molecular weight is very similar among the samples and remain at ca. 3060–5900 g mol^{-1}. These values can be associated to polymer chains formed by 6–11 repetitive units according with the specific value assumed, M_n or M_w, respectively.

Figure 3 shows SEC traces for the polymers. In all cases, the shape of the curve is associated to a unimodal material, with an average polydispersity index (M_w/M_n) between 1.67 and 1.78, which is expected for polycondensation polymers.

Because the purity of the monomers and the employed molar relationship between them in the polycondensation process were strongly controlled, a possible explanation for these results is the low mobility of the growing chains in the reaction medium. Similar results were reported by us for the synthesis of polyamides using these silylated acid chlorides and also their diacid derivatives with several aromatic diamines. For these last reactions, Yamazaki-Higashi polycondensation technique was again employed.[24–26]

Solubility essays were accomplished at room temperature (ca. 25 °C) using 1 mg of polymer in 1 mL of solvent. New thiophene-containing polymers exhibit high solubility in aprotic polar solvents such as DMSO, DMF, NMP, DMAc, and *m*-cresol, even in low boiling point solvents such as THF and $CHCl_3$. All samples were insoluble in water, acetone and alcohols of low molecular weight. The nonplanar 3D structure of the diamine monomer

Table II. Thermal and optical results of poly(amide)s

	Thermal properties				Optical properties			
	$TDT_{10\%}$[a] (°C)	$T^{g,b}$ (°C)	R_{700}[c] (%)	LOI[d] (%)	$T_{80\%}$[e] (nm)	$\lambda_{cut\ off}$[f] (nm)	E_g^{optg} (eV)	λ_{max}[h] (nm)
P(AT-MMSi)	439	157	38	32.7	427	373	3.2	452
P(AT-MPSi)	442	159	48	36.7	424	371	3.2	444
P(AT-PPSi)	461	178	50	37.5	427	373	3.3	447

[a] Thermal decomposition temperature at which 10% weight loss.
[b] Glass transition temperature taken from the second heating scan.
[c] Residual weight when heated at 600 °C.
[d] Limiting oxygen index calculated as LOI = 17.5 + 0.4 (Rw_{800}).
[e] 80% transmittance wavelength.
[f] Cut off wavelength.
[g] Band-gap values taken from UV-vis spectra.
[h] Emission maximum taken from photoluminescence spectra.

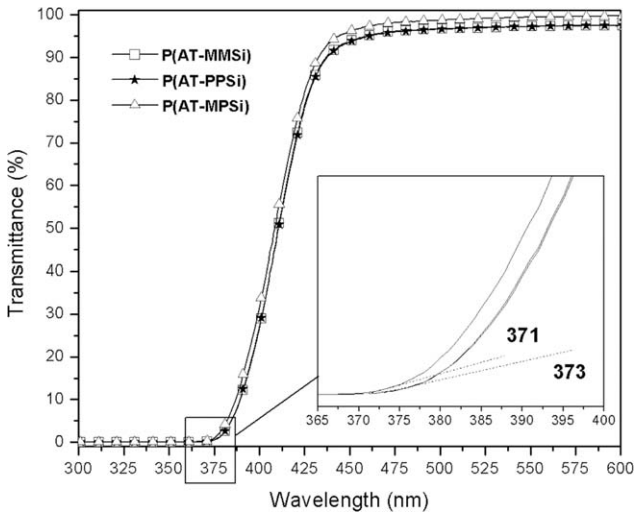

Figure 5. UV-vis optical transmission spectra of the thiophene- and silicon-containing polyamides.

could promote the formation of less regular polymers, which affects the intermolecular interactions and provides more flexibility to the chains. This behavior would allow an adequate processability of the materials and the easy preparation of thin films.

Thermal Studies

Figure 4 shows the thermal degradation profiles and DSC curves obtained under nitrogen atmosphere by thermogravimetric analysis (TGA) and differential scanning calorimetry (DSC), respectively. The glass transition temperatures (T_g), 10% of mass loss thermal decomposition temperatures ($TDT_{10\%}$) and residual weight ratio at 800 °C (R_{800}) are reported in Table II. The effect of the molecular weight variations on these properties should be disregarded considering the already discussed SEC results.

TGA analysis evidenced that all polymers present a starting decomposition temperature above 350 °C and the $TDT_{10\%}$ values are above 430 °C. In agreement with the general idea that a polymer is considered as thermostable when its weight loss is less than 10% at 400 °C, the synthesized oligomers can be considerate as thermally stable materials. Derivative curves (inset Figure 4) for the three PAs showed a common process of high decomposition rate centered at 465 °C. A second maximum centered at 513 °C is observed for **P(AT-MMSi),** which shifts toward higher temperature (555 °C) for the other two samples. This second thermal process would be associated to aromatic rings decomposition. **P(AT-PPSi)** presents higher $TDT_{10\%}$ value than **P(AT-MMSi)** and **P(AT-MPSi),** probably due to its higher aromatic content.

Residual weight ratios at 800 °C are between 38–50% being higher for **P(AT-PPSi),** in agreement with its higher aromatic content. The nature of these residues probably corresponds to silicon oxides formed during the heating process. Limiting oxygen index (LOI) calculated from Kreveler equation (Table II)[13,36] showed values above to the established limit (20.9%) with an average of 35.6%. Accordingly, all polyamides do not burn easily in air and present a low trend to propagate flame when the igniting source is removed.

DSC analyses showed T_g values between ca. 160 °C and 180 °C (Table II). Again, **P(AT-PPSi)** exhibits the highest T_g value. This fact would indicate that the replacement of methyl groups by phenyl ones on the silicon atom reduces the flexibility of the chain backbone. The presence of two phenyl group as side elements would increase the free rotation energy of the C—Si bonds in the main chain. The same trend has been verified in previous studies for several silylated-condensation polymers.[24–26,37,38]

Optical Properties

Figure 5 depicts the results of UV-vis optical transparency studies at 25 °C for silylated-polyamides using NMP solutions (5 mg sample in 1 mL solvent). All polyamides show similar profiles. Although the transmittance value to 400 nm is low, at about 430 nm this parameter is higher than 90% with an average transmittance over 95% in the visible region. Besides, the cut off values are very near without showing a significant variation with regard to the substituted groups on the silicon atom (Table II). Probably, the difference in the flexibility evidenced from the DSC analysis is not enough to affect the packing forces when the chains are in solution and, therefore, the transmittance results are similar.

UV-vis absorption spectra of ~1 mg PA in 1 mL of THF samples are seen in Figure 6(a). The three PAs present strong absorption bands close to 300 nm, which can be ascribed to π-π^* benzenoid electronic transitions.[31,34,39–41] Between 400–

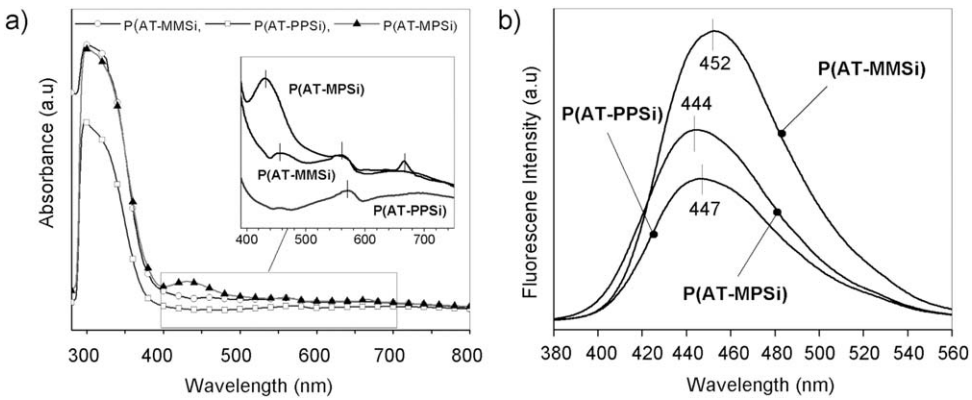

Figure 6. UV-vis absorption spectra (a) and fluorescence emission spectra (b) of the PAs.

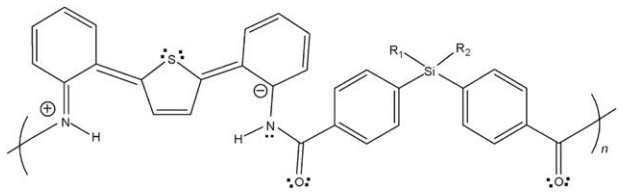

Figure 7. Representation of quinoid type structure of the thiophene-dianiline unit.

500 nm, low intensity absorption bands for **P(AT-MMSi)** and **P(AT-PPSi)** and medium intensity absorption band for **P(AT-MPSi)** are found [inset, Figure 6(a)]. The presence of these bands could indicate the formation of mesomeric quinoid structures along the polymer chains. It has been reported that polyanilines prepared from *o*-phenylenediamine[39–41] show an absorption band in the same region of the UV-vis spectrum. The authors ascribed this band to n-π^* transitions between the quinoid ring and nonbonding orbitals of nitrogen atom of the $-NH_2$ groups. The presence of *o*-quinoid type structures on aniline ring would be a consequence of the great ability of the neighboring thiophene ring to adopt a quinoid resonant form.[42]

The absorption bands above 550 nm evidences the conjugation extent along the main chain and reflects the electronic charge delocalization induced by the thiophene-dianiline unit (Figure 7). However, the low intensity of these bands reflects the punctual and isolated formation of this type of structures. On the other hand, molecular weights similarity leads to disregard its effect on the discussed optical and electronic properties.

The magnitude of the optical band-gap (E_g^{opt}) of each sample was estimated from the UV-vis spectrum using the following equation:

$$E_g^{opt} = \frac{hc}{\lambda_{max}} = \frac{1,242}{\lambda_{max}} \text{ eV}$$

where λ_{max} is the value of the intersection between the tangential line through the inflection point of the absorption band of higher intensity and the baseline set at $y = 0$.[31]

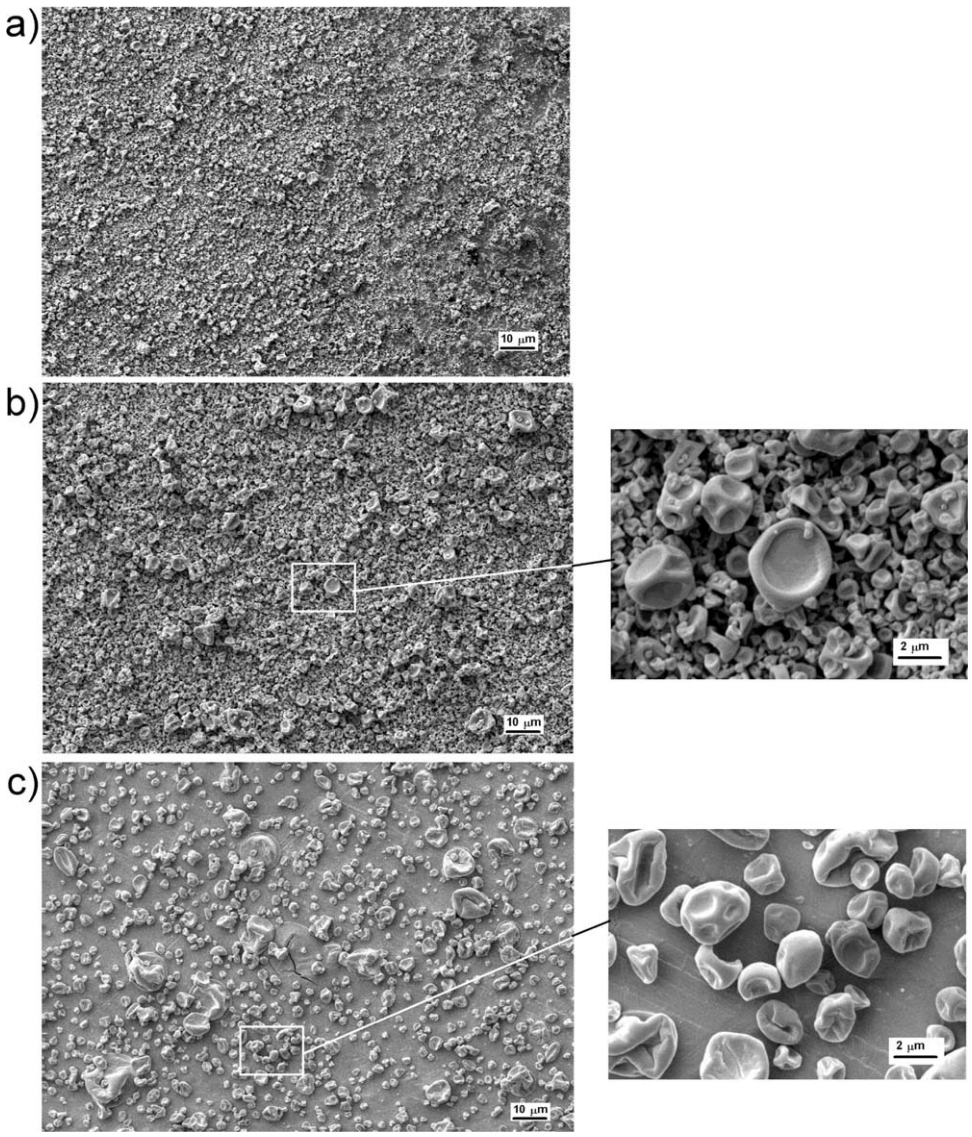

Figure 8. Surface topography for (a) **P(AT-MMSi)** (2,000×); (b) **P(AT-PPSi)** (2,000× and 15,000×), and (c) **P(AT-MPSi)** (2,000× and 15,000×).

No significant differences between E_g^{opt} values are observed (Table II). Thus, the symmetry/asymmetric effect of the substitutions on the silicon atom does not affect this parameter. The major contribution of π-π^* benzenoid electronic transitions of independent and nonconjugated monomer units explain these results. The high E_g^{opt} values (ca. 3.2 eV) suggest, as expected, a limited π-conjugation along the polymer backbone leading to classify these PAs as insulating materials.

Figure 6(b) shows the fluorescence emission spectra of PAs. It can be seen that the emission maxima of the three samples are close to 450 nm in the blue region of the electromagnetic spectrum. The blue-emitting materials are potential candidates for use in optoelectronics and optoelectronic devices such as tunable lasers and amplifers, optical fibers and electroluminescent devices.[43]

Scanning Electron Microscopy (SEM)

Topography at surface level of polymer samples was examined using SEM at different magnifications. Polymer solution (30 mg dissolved in 200 μL THF) and high voltage applied, through electrospinning technique (20 kV), were varied in order to generate nanostructure arrangements for each sample.

The results show that the depositions shape obtained are not of fibrous nature (Figure 8). This fact is probably due to the low molecular weight of the samples. As PAs present very similar molecular weights and the only structural difference is centered in the radical groups bonded to the silicon atom (Scheme 3), the self-organized structures generation would be related to the structural symmetry of each polymer.

Films composed by **P(AT-MMSi)** showed small monodispersed rounded particles related to higher surface density [Figure 8(a)]. In Figure 8(b) is possible to detect the same morphology with a well-defined structure and size near to 2.5–4.5 μm, dimensions that could be related to steric effect of the phenyl group already discussed. On the background, smaller particles are observed, with dimensions that vary between 0.8–1.0 μm (right side Figure 8(b) obtained at 15,000 X). Both samples **P(AT-MMSi)** and **P(AT-PPSi)** present a unique morphology, due to the symmetry of the repetitive units, which was spontaneously formed when the voltage was applied. On the other hand, when the polymeric structure shows asymmetry (**P(AT-MPSi)**), rounded particles are also observed with dimensions that vary from 1.5 to 3.5 μm [Figure 8(c)]. In this case, it is possible to detect a smooth polymer surface on the background. This effect is probably produced by higher interchain interactions producing bigger structures at surface level. The particles are not completely spherical having a certain concavity. This fact would be associated to the vacuum generated by the SEM technique, which promotes solvent evaporation leading to microstructure collapse.

CONCLUSIONS

Three new polyamides based on organosilane and thiophene-dianiline monomers were synthesized in good yields. Polymer structure was corroborated by elemental analysis and spectroscopic methodologies. Inherent viscosity (η_{inh}) values and SEC results are indicatives of low and similar molecular weight materials with chains formed by 6–11 repetitive units. Besides, the polymers exhibited excellent solubility in common organic solvents and low boiling points solvents. All polyamides were thermally stable. The high aromatic content explains why **P(AT-PPSi)** shows the highest thermal stability and also the highest T_g value of the series. However, the transparency in the UV-visible region, the band-gap and the fluorescence emission maxima are similar for all samples. Although the monomers are $\pi-$conjugated systems, there is no effective overlapping between their orbitals, hence only limited charge transfers occurs along the polymer chains. The high E_g^{opt} values support this explanation. Molecule symmetry and the high voltage applied to deposit the polymer over the substrate by electrospun technique, produced spherical particles with certain concavity from symmetrical polymers with high spatial and geometric homogeneity. These results showed that this methodology is appropriate to form ordered structures at surface level.

ACKNOWLEDGMENTS

I. A. Jessop acknowledges the financial support by Comisión Nacional de Investigación Científica y Tecnológica CONICYT through project FONDECYT POSTDOCTORADO No. 3140609. A. Tundidor-Camba acknowledges the financial assistance by CONICYT through Project 79130011. Likewise, authors thank to FONDECYT No. 11121281 for electrospinning sample deposition and to Universidad Tecnológica Metropolitana (UTEM) for sputter coater acquisition.

REFERENCES

1. Alvi, M. U.; Zulfiqar, S.; Yavuz, C. T.; Kweon, H.-S.; Sarwar, M. I. *Ind. Eng. Chem. Res.* **2013**, *52*, 6908.
2. Kim, H. J.; Choi, K.; Baek, Y.; Kim, D.-G.; Shim, J.; Yoon, J.; Lee, J.-C. *ACS Appl. Mater. Interfaces* **2014**, *6*, 2819.
3. Cassidy, P. E. Thermally Stable Polymers; Dekker: New York, **1980**.
4. Yang, H. H. Aromatic High-Strength Fibers; Wiley: New York, **1989**.
5. Seymour, R. B.; Carraher, C. E. Polymer Chemistry: An Introduction, 2nd ed.; Dekker: New York, **1988**.
6. García, J. M.; García, F. C.; Serna, F.; de la Peña, J. L. *Prog. Polym. Sci.* **2010**, *35*, 623.
7. Bera, D.; Padmanabhan, V.; Banerjee, S. *Macromolecules* **2015**, *48*, 4541.
8. Sava, I.; Iosip, M.-D.; Bruma, M.; Hamciuc, C.; Robison, J.; Okrasa, L.; Pakula, T. *Eur. Polym. J.* **2003**, *39*, 725.
9. Yoshioka, Y. *Colloid Polym. Sci.* **2013**, *291*, 1641.
10. Liu, X.-L.; Wu, D.; Sun, R.; Yu, L.-M.; Jiang, J.-W.; Sheng, S.-R. *J. Fluorine Chem.* **2013**, *154*, 16.
11. Wu, J.; Jasinska-Walc, L.; Dudenko, D.; Rozanski, A.; Hansen, M. R.; van Es, D.; Koning, C. E. *Macromolecules* **2012**, *45*, 9333.
12. Bandyopadhyay, P.; Banerjee, S. *Ind. Eng. Chem. Res.* **2014**, *53*, 18273.
13. Mallakpour, S.; Zadehnazari, A. *J. Adv. Res.* **2014**, *5*, 311.

14. Guo, F.; Servi, A.; Liu, A.; Gleason, K. K.; Rutledge, G. C. *ACS Appl. Mater. Interfaces* **2015**, *7*, 8225.
15. Mercante, L. A.; Pavinatto, A.; Iwaki, L. E. O.; Scagion, V. P.; Zucolotto, V.; Oliveira, O. N.; Mattoso, L. H. C. Jr.; Correa, D. S. *ACS Appl. Mater. Interfaces* **2015**, *7*, 4784.
16. Stachewicz, U.; Barber, A. H. *Langmuir* **2011**, *27*, 3024.
17. Jordan, A. M.; Korley, L. T. J. *Macromolecules* **2015**, *48*, 2614.
18. Valiquette, D.; Pellerin, C. *Macromolecules* **2011**, *44*, 2838.
19. Dhakate, S. R.; Singla, B.; Uppal, M.; Mathur, R. B. *Adv. Mater. Lett.* **2010**, *1*, 200.
20. Song, K.; Wu, Q.; Zhang, Z.; Ren, S.; Lei, T.; Negulescu, I. I.; Zhang, Q. *ACS Appl. Mater. Interfaces* **2015**, *7*, 15108.
21. Li, D.; Xia, Y. *Adv. Mater.* **2004**, *16*, 1151.
22. Wu, J.; Wang, N.; Zhao, Y.; Jiang, L. *J. Mater. Chem. A* **2013**, *1*, 7290.
23. Hou, H.; Wang, L.; Gao, F.; Wei, G.; Tang, B.; Tang, W.; Wu, T. *J. Am. Chem. Soc.* **2014**, *136*, 16716.
24. Tundidor-Camba, A.; Terraza, C. A.; Tagle, L. H.; Coll, D. *J. Appl. Polym. Sci.* **2011**, *120*, 2381.
25. Tagle, L. H.; Terraza, C. A.; Leiva, A.; Devilat, F. *J. Appl. Polym. Sci.* **2008**, *110*, 2424.
26. Terraza, C. A.; Tagle, L. H.; Mejías, D.; Tundidor-Camba, A.; Ortiz, P.; Muñoz, D.; Alvarez, F.; González-Henríquez, C. M. *Polym. Bull.* **2013**, *70*, 773.
27. González-Henríquez, C. M.; Terraza, C. A.; Tagle, L. H.; Barriga-González, A.; Volkmann, U. G.; Cabrera, A. L.; Ramos-Moore, E.; Retamal, M. J. *J. Mater. Chem.* **2012**, *22*, 6782.
28. Terraza, C. A.; Tagle, L. H.; Tundidor-Camba, A.; González-Henríquez, C. M.; Ortiz, P.; Coll, P. *Eur. Polym. J.* **2012**, *48*, 649.
29. González-Henríquez, C. M.; Tagle, L. H.; Terraza, C. A.; Barriga-González, A.; Volkmann, U. G.; Cabrera, A. L.; Ramos-Moore, E.; Pavez-Moreno, M. *Polym. Int.* **2012**, *61*, 197.
30. Terraza, C. A.; Tagle, L. H.; Muñoz, D.; Tundidor-Camba, A.; Ortiz, P. A.; Coll, D.; González-Henríquez, C. M.; Jessop, I. A. *Polym. Bull.* **2016**, *73*, 1103.
31. Jessop, I. A.; Zamora, P. P.; Díaz, F. R.; del Valle, M. A.; Leiva, A.; Cattin, L.; Makha, M.; Bernède, J. C. *Int. J. Electrochem. Sci.* **2012**, *7*, 9502.
32. Thompson, A. E.; Hughes, G.; Batsanov, A. S.; Bryce, M. R.; Parry, P. R.; Tarbit, B. *J. Org. Chem.* **2005**, *70*, 388.
33. Tagle, L. H.; Terraza,; Ahlers, W.; Vera, C. *J. Chil. Chem. Soc.* **2005**, *50*, 535.
34. Jessop, I. A.; Zamora, P. P.; Díaz, F. R.; del Valle, M. A.; Bernède, J. C. *J. Chil. Chem. Soc.* **2014**, *59*, 2394.
35. Terraza, C. A.; Tagle, L. H.; Concha, F.; Poblete, L. *Des. Monomers Polym.* **2007**, *10*, 253.
36. van Krevelen, D. W.; Hofyzer, P. J. Properties of Polymers, 2nd ed.; Elsevier: Amsterdam, **1976**.
37. Tagle, L. H.; Terraza, C. A.; Leiva, A.; Valenzuela, P. *J. Appl Polym. Sci.* **2006**, *102*, 2768.
38. Terraza, C. A.; Tagle, L. H.; Leiva, A.; Poblete, L.; Concha, F. C. *J. Appl. Polym. Sci.* **2008**, *109*, 303.
39. Archana, S.; Shanti, J. *Res. J. Chem. Sci.* **2014**, *4*, 60.
40. Sayyah, S. M.; Khaliel, A. B.; Aboud, A. A.; Mohamed, S. M. *Int. J. Polym. Sci.* **2014**, *520910*, 1.
41. Huang, M. R.; Li, X.-G.; Duan, W. *Chem. Rev.* **2009**, *109*, 5868.
42. Roncali, J. *Chem. Rev.* **1997**, *97*, 173.
43. Patil, S. R.; Shelar, D. P.; Rote, R. V.; Jachak, M. N. *J. Fluoresc.* **2011**, *21*, 2037.